Precision Measurement of the Λ_b^0 Baryon Lifetime

R. Aaij *et al.**
(LHCb Collaboration)

(Received 9 July 2013; published 5 September 2013)

The ratio of the Λ_b^0 baryon lifetime to that of the $\bar{B}^0$ meson is measured using 1.0 fb^{-1} of integrated luminosity in 7 TeV center-of-mass energy pp collisions at the LHC. The Λ_b^0 baryon is observed for the first time in the decay mode $\Lambda_b^0 \to J/\psi p K^-$, while the $\bar{B}^0$ meson decay used is the well known $\bar{B}^0 \to J/\psi \pi^+ K^-$ mode, where the $\pi^+ K^-$ mass is consistent with that of the $\bar{K}^{*0}(892)$ meson. The ratio of lifetimes is measured to be $0.976 \pm 0.012 \pm 0.006$, in agreement with theoretical expectations based on the heavy quark expansion. Using previous determinations of the $\bar{B}^0$ meson lifetime, the Λ_b^0 lifetime is found to be $1.482 \pm 0.018 \pm 0.012$ ps. In both cases, the first uncertainty is statistical and the second systematic.

DOI: 10.1103/PhysRevLett.111.102003 PACS numbers: 13.30.Eg, 14.20.Mr

Evaluations from experimental data of fundamental parameters, such as Cabibbo-Kobayashi-Maskawa (CKM) matrix elements [1], and limits on physics beyond that described by the standard model, often rely on theoretical input [2]. One of the most useful models, the heavy quark expansion (HQE) [3–5], is based on the operator product expansion [6]; it is used, for example, to extract values for $|V_{ub}|$ and $|V_{cb}|$ from measurements of inclusive semileptonic B meson decays [7]. In the free quark model, the lifetimes of all b-flavored hadrons are equal, because the decay width is determined by the b quark lifetime. This model is too naïve, since effects of other quarks in the hadron are not taken into account [8]. Early predictions using the HQE, however, supported the idea that b-hadron lifetimes were quite similar, due to the absence of correction terms $O(1/m_b)$. In the case of the ratio of lifetimes of the Λ_b^0 baryon, $\tau_{\Lambda_b^0}$, to the $\bar{B}^0$ meson, $\tau_{\bar{B}^0}$, the corrections of order $O(1/m_b^2)$ were found to be small, initial estimates of $O(1/m_b^3)$ [9,10] effects were also small, thus, differences of only a few percent were expected [8,9,11]. Measurements at LEP, however, indicated that $\tau_{\Lambda_b^0}/\tau_{\bar{B}^0}$ was lower: in 2003 one widely quoted average of all data gave 0.798 ± 0.052 [12], while another gave 0.786 ± 0.034 [13]. Some authors sought to explain the small value of the ratio by including additional operators or other modifications [14], while others thought that the HQE could be pushed to provide a ratio of ~ 0.9 [15]. Recent measurements have shown indications that a higher value is possible [16], although the uncertainties are still large. Therefore, a precision measurement of $\tau_{\Lambda_b^0}/\tau_{\bar{B}^0}$ is necessary to provide a confirmation of the HQE, or show definitively that the theory is deficient.

In this Letter, we present the experimental determination of $\tau_{\Lambda_b^0}/\tau_{\bar{B}^0}$ using a data sample corresponding to 1.0 fb^{-1} of integrated luminosity accumulated by the LHCb experiment in 7 TeV center-of-mass energy pp collisions. The Λ_b^0 baryon is detected in the $J/\psi p K^-$ decay mode, while the $\bar{B}^0$ meson is found in $J/\psi \pi^+ K^-$ decays. Mention of a particular decay channel implies the additional use of the charge-conjugate mode. This Λ_b^0 decay mode has not been observed before. (Measurement of the branching fraction is under study, and will be reported in a subsequent publication.) On the other hand, the $\bar{B}^0$ decay is well known, and we impose the further requirement that the invariant mass of the $\pi^+ K^-$ combination be within ± 100 MeV of the $\bar{K}^{*0}(892)$ mass (we work in units where $c = 1$) in order to simplify the simulation and reduce systematic uncertainties. These decays have the same decay topology into four charged tracks, thus, facilitating the cancellation of uncertainties.

The LHCb detector is a single-arm forward spectrometer covering the pseudorapidity range $2 < \eta < 5$, described in detail in Ref. [17]. Events selected for this analysis are triggered [18] by a $J/\psi \to \mu^+ \mu^-$ decay, where the J/ψ is required at the software level to be consistent with coming from the decay of a b hadron by use either of impact parameter (IP) requirements or detachment of the J/ψ from the associated primary vertex. The simulated events used in this analysis are produced using the software described in Ref. [19].

Events are preselected and then are further filtered using a multivariate analyzer based on the boosted decision tree (BDT) technique [20]. In the preselection, all hadron track candidates are required to have p_T larger than 250 MeV, while for muon candidates, the requirement is more than 550 MeV. Events must have a $\mu^+ \mu^-$ combination that forms a common vertex with $\chi^2 < 16$, and an invariant mass between -48 and $+43$ MeV of the J/ψ mass. Candidate $\mu^+ \mu^-$ combinations are then constrained to the J/ψ mass for subsequent use in event selection. The two charged final state hadrons must have a vector summed

*Full author list given at end of the article.

p_T of more than 1 GeV, and are also required to form a vertex with $\chi^2 < 10$ for one degree of freedom, and a common vertex with the J/ψ candidate with $\chi^2 < 50$ for five degrees of freedom. This b-hadron candidate must have a momentum vector that, when parity inverted, points to the primary vertex within an angle smaller than 2.56°. Particle identification requirements differ in the two modes. We use the difference in the logarithm of the likelihood, DLL($h_1 - h_2$), to distinguish between the two hypotheses: h_1 and h_2 as described in [21]. In the Λ_b^0 decay, the kaon candidate must have DLL($K - \pi$) > 4 and DLL($K - p$) > −3, while the proton must have DLL($p - \pi$) > 10 and DLL($p - K$) > −3. For the $\bar{B}^0$ decay, the requirements on the pion candidate are DLL($\pi - \mu$) > −10 and DLL($\pi - K$) > −10, while DLL($K - \pi$) > 0 is required for the kaon.

The BDT selection is based on the minimum DLL($\mu - \pi$) of the μ^+ and μ^- candidates, the p_T of each of the two charged hadrons, and their sum, the $\Lambda_b^0 p_T$, the Λ_b^0 vertex χ^2, and the impact parameter χ^2 of the Λ_b^0 candidate, where the latter results from calculating the difference in χ^2 by using the hypothesis that the IP is zero. These variables are chosen with the aim of having the selection efficiency be independent of decay time. The BDT is trained on a simulated sample of either $\Lambda_b^0 \to J/\psi p K^-$ signal events and a background data sample from the mass sidebands of the Λ_b^0 signal peak. It is then tested on independent samples from the same sources. The BDT selection is implemented to maximize $S^2/(S + B)$, where S indicates the signal and B the background event yields. This optimization includes the requirement that the Λ_b^0 baryon decay time be greater than 0.5 ps. The same BDT selection is used for the $\bar{B}^0 \to J/\psi \pi^- K^+$ mode.

The $J/\psi p K^-$ mass distribution after the BDT selection is shown in Fig. 1. There is a large and significant signal. Backgrounds can be combinatorial in nature, but can also be formed by reflections from B meson decays where the particle identification fails. As long as these backgrounds do not peak near the Λ_b^0 mass they cannot cause incorrect determinations of the Λ_b^0 signal yield. The shapes of the main B meson reflections are determined from simulation and shown in Fig. 1. The shapes are smooth and do not peak in the signal region. To estimate the contributions of the reflections, we take each of the candidates in the $J/\psi p K^-$ sideband regions 60–200 MeV on either side of the Λ_b^0 mass peak, reassign proton to kaon and pion mass hypotheses, respectively, and fit the resulting signal peaks determining signal yields of 5576 ± 95 $\bar{B}_s^0$ and 1769 ± 192 $\bar{B}^0$ decays. To translate these yields to those within ±20 MeV of the Λ_b^0 peak, we use simulations of $\bar{B}_s^0 \to J/\psi K^+ K^-$ with the $K^+ K^-$ mass distribution matched to that obtained in our previous analysis of this final state [22], and a simulation of $\bar{B}^0 \to J/\psi \pi^+ K^-$ decays, leading to 1186 ± 35 $J/\psi K^+ K^-$ and 308 ± 33 $J/\psi \pi^+ K^-$ reflected decays, respectively.

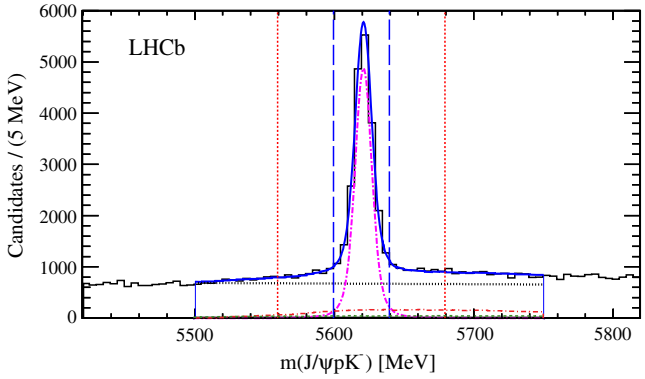

FIG. 1 (color online). Invariant mass spectrum of $J/\psi p K^-$ combinations. The signal region is between the vertical long dashed (blue) lines. The sideband regions extend from the dotted (red) lines to the edges of the plot. The fit to the data between 5500 and 5750 MeV is also shown by the (blue) solid curve, with the Λ_b^0 signal shown by the dashed-dotted (magenta) curve. The dotted (black) line is the combinatorial background and $\bar{B}_s^0 \to J/\psi K^+ K^-$ and $\bar{B}^0 \to J/\psi \pi^+ K^-$ reflections are shown with the dashed-double-dotted (red) and dashed (green) shapes, respectively.

To determine the Λ_b^0 signal yield, we perform an unbinned maximum likelihood fit to the $J/\psi p K^-$ invariant mass spectrum shown in Fig. 1 in the region between 5500 and 5750 MeV. The fit function is the sum of the Λ_b^0 signal component, combinatorial background, and the contribution from the $\bar{B}_s^0 \to J/\psi K^+ K^-$ and $\bar{B}^0 \to J/\psi \pi^+ K^-$ reflections. The signal is modeled by a triple-Gaussian function with common means; the effective rms width is 5.5 MeV. The combinatorial background is described by an exponential function. The event yields of the reflections are included in the fit as Gaussian constraints. The mass fit gives 15 581 ± 178 signal and 5535 ± 50 combinatorial background candidates together with 1235 ± 35 $\bar{B}_s^0 \to J/\psi K^+ K^-$ and 313 ± 26 $\bar{B}^0 \to J/\psi \pi^+ K^-$ reflection candidates within ±20 MeV of the Λ_b^0 mass peak.

To view the background subtracted pK^- mass spectrum, we perform fits, as described above, to the $m(J/\psi p K^-)$ distributions in bins of $m(pK^-)$ and extract the signal yields within ±20 MeV of the Λ_b^0 mass peak. The resulting pK^- mass spectrum is shown in Fig. 2. A distinct peak is observed in the pK^- invariant mass distribution near 1520 MeV, together with the other resonant and nonresonant structures over the entire kinematical region. The peak corresponds to the $\Lambda(1520)$ resonance [23]. Simulations of the Λ_b^0 decay are weighted to reproduce this mass distribution.

The $J/\psi \pi^+ K^-$ mass spectrum, after the BDT selection, is shown in Fig. 3. There is a large signal peak at the $\bar{B}^0$ mass and a much smaller one at the $\bar{B}_s^0$ mass. Triple-Gaussian functions, each with common means, are used to fit the signal peaks; the effective rms width is 6.7 MeV. An exponential function is used to fit the combinatorial background.

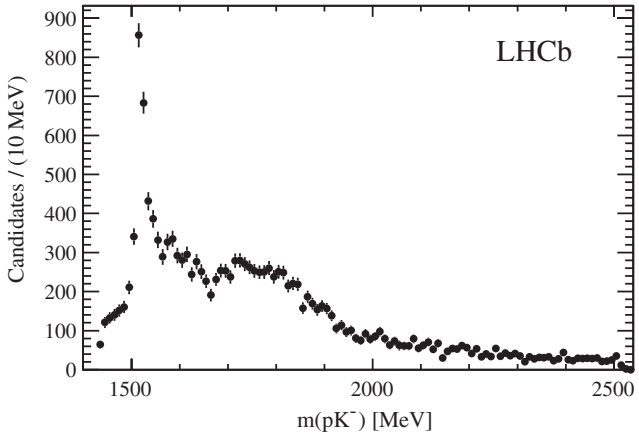

FIG. 2. Background subtracted $m(pK^-)$ distribution obtained by fitting the $m(J/\psi pK^-)$ distribution in bins of $m(pK^-)$.

The mass fit gives $97\,506 \pm 447$ signal and 3660 ± 74 background candidates within ± 20 MeV of the $\bar{B}^0$ mass peak. Reflections are possible from both $\bar{B}_s^0 \to J/\psi K^+ K^-$ and $\Lambda_b^0 \to J/\psi p K^-$ decays. Following the same procedure as outlined above using the sidebands of the $\bar{B}^0$ signal, we find no evidence of a reflection from the $\bar{B}_s^0$ state and a small, nonpeaking, contribution of 506 ± 19 events from the Λ_b^0 state, in the $\bar{B}^0$ signal region, that is ignored.

The decay time for each candidate is given by $t = m\vec{d} \cdot \vec{p}/|\vec{p}|^2$, where m is the mass, $\vec{d}$ the distance vector from the primary vertex to the decay point, and $\vec{p}$ is the measured b hadron momentum. Here, we do not constrain the two muons to the J/ψ mass to avoid systematic biases. The decay time resolutions are 40 fs for the Λ_b^0 decay and 37 fs for the $\bar{B}^0$ decay. In addition, the decay time acceptances are also almost equal. For equal acceptances, the ratio of events, $R(t)$, as a function of decay time is given by

$$R(t) = \frac{N_{\Lambda_b^0}(0)}{N_{\bar{B}^0}(0)} \frac{e^{-t/\tau_{\Lambda_b^0}}}{e^{-t/\tau_{\bar{B}^0}}} = R(0) e^{-t\Delta_{\Lambda B}}, \quad (1)$$

where $\Delta_{\Lambda B} = (1/\tau_{\Lambda_b^0} - 1/\tau_{\bar{B}^0})$. Effects of the different decay time resolutions in the two modes are negligible above 0.5 ps. First order corrections for a decay time dependent acceptance ratio can be taken into account by modifying Eq. (1) with a linear function

$$R(t) = R(0)[1 + at] e^{-t\Delta_{\Lambda B}}, \quad (2)$$

where a represents the slope of the acceptance ratio as a function of decay time.

The decay time acceptances for both modes are determined by simulations that are weighted to match either the pK^- or $\pi^+ K^-$ invariant mass distributions seen in data, as well as to match the measured p and p_T distributions of the b hadrons. In addition, we further weight the samples so that the simulation matches the hadron identification efficiencies obtained from $D^{*+} \to \pi^+ (D^0 \to \pi^+ K^-)$ events for pions and kaons, and $\Lambda^0 \to p\pi^-$ for protons.

The ratio of the decay time acceptances is shown in Fig. 4. Here, we have removed the minimum requirement on decay time so we can view the distributions in the region close to zero time. The individual acceptances in both cases can be described with a linear function above 0.5 ps. In order to minimize possible systematic effects, we use candidates with decay times larger than 0.6 ps. We also choose an upper time cut of 7.0 ps, because the acceptance is poorly determined beyond this value. The acceptance ratio is fitted with a linear function between 0.6 and 7.0 ps. The slope is $a = 0.0033 \pm 0.0024$ ps^{-1}, and the χ^2/number of degrees of freedom (NDF) of the fit is 81/62.

We determine the event yields in both decay modes by fitting the invariant mass distributions in 16 bins of decay time, each bin 0.4 ps wide, using the same signal and

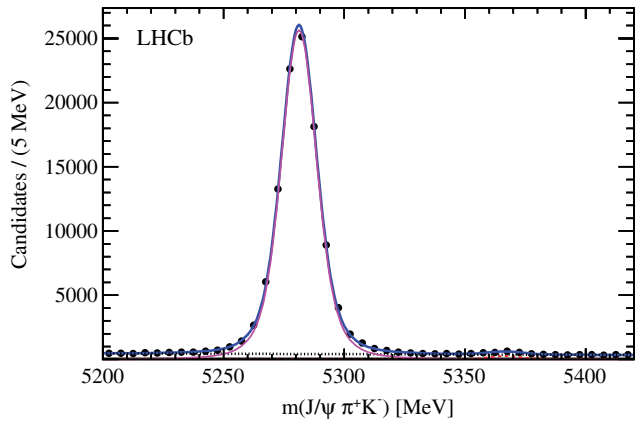

FIG. 3 (color online). Fit to the invariant mass spectrum of $J/\psi \pi^+ K^-$ combinations with $\pi^+ K^-$ invariant mass within ± 100 MeV of the $\bar{K}^{*0}$ mass. The $\bar{B}^0$ signal is shown by the solid (magenta) curve, the combinatorial background by the dotted (black) line, the $\bar{B}_s^0 \to J/\psi \pi^+ K^-$ signal by the dashed (red) curve, and the total by the solid (blue) curve.

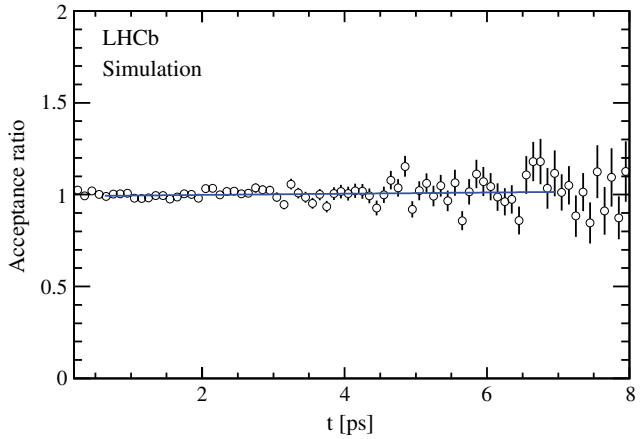

FIG. 4 (color online). Ratio of the decay time acceptances between $\Lambda_b^0 \to J/\psi p K^-$ and $\bar{B}^0 \to J/\psi \bar{K}^{*0}(892)$ decays obtained from simulation. The solid (blue) line shows the result of the linear fit.

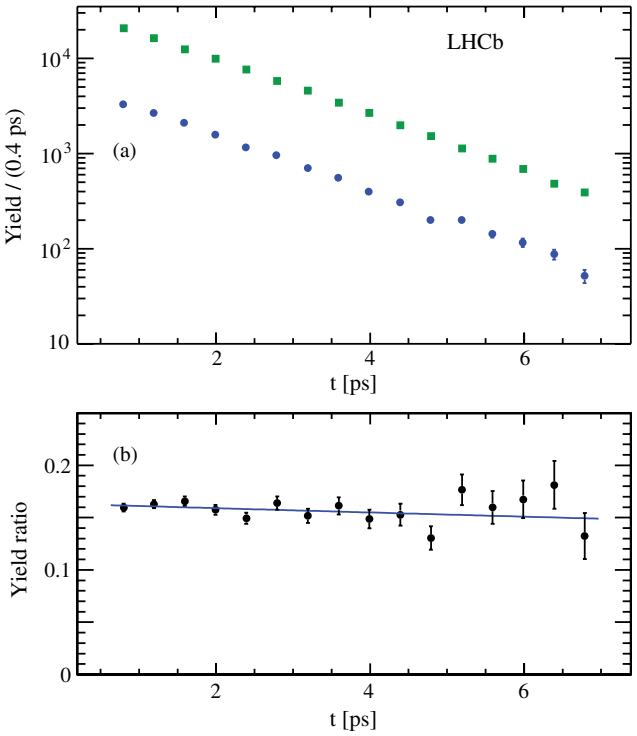

FIG. 5 (color online). (a) Decay time distributions for $\Lambda_b^0 \to J/\psi p K^-$ shown as (blue) circles, and $\bar{B}^0 \to J/\psi \bar{K}^{*0}(892)$ decays shown as (green) squares. For most entries the error bars are smaller than the points. (b) Yield ratio of $\Lambda_b^0 \to J/\psi p K^-$ to $\bar{B}^0 \to J/\psi \bar{K}^{*0}(892)$ events fitted as a function of decay time.

background shapes obtained in the aforementioned mass fits. Since the bin size is approximately ten times the resolution, there is no effect due to the small difference of time resolution ($< 7\%$) between the two modes. The resulting distributions are shown in Fig. 5(a). Here, the fitted signal yields in both modes are placed at the average of the decay time within a bin determined by the $\bar{B}^0$ data in order to correct for the exponential decrease of the decay time distributions across the bin. The decay time ratio distribution fitted with the function given in Eq. (2) is shown in Fig. 5(b). The χ^2/NDF of the fit is 18/14, with a p value of 21%. The fitted value of the reciprocal lifetime difference is

$$\Delta_{\Lambda B} = 16.4 \pm 8.2 \pm 4.4 \text{ ns}^{-1}.$$

Whenever two uncertainties are quoted, the first is the statistical and the second systematic; the latter will be discussed below. Numerically, the ratio of lifetimes is

$$\frac{\tau_{\Lambda_b^0}}{\tau_{\bar{B}^0}} = \frac{1}{1 + \tau_{\bar{B}^0}\Delta_{\Lambda B}} = 0.976 \pm 0.012 \pm 0.006,$$

where we use the world average value $\tau_{\bar{B}^0} = 1.519 \pm 0.007$ ps [23]. Multiplying the lifetime ratio by this value, we determine

$$\tau_{\Lambda_b^0} = 1.482 \pm 0.018 \pm 0.012 \text{ ps}.$$

TABLE I. Absolute systematic uncertainties on $\Delta_{\Lambda B}$, the lifetime ratio, and the Λ_b^0 lifetime.

Source	$\Delta_{\Lambda B}$ (ns^{-1})	$\tau_{\Lambda_b^0}/\tau_{\bar{B}^0}$	$\tau_{\Lambda_b^0}$ (fs)
Decay time fit range	3.2	0.0045	6.9
Acceptance slope	2.3	0.0033	5.0
Signal shape	1.4	0.0021	3.2
Background model	1.2	0.0017	2.6
pK helicity	0.1	0.0002	0.2
Acceptance function	0.1	0.0001	0.2
$\bar{B}^0$ lifetime	...	0.0001	6.8
Total	4.4	0.0062	11.7

Our result is consistent with, but higher and more accurate than, the current world average of 1.429 ± 0.024 ps [23].

The absolute systematic uncertainties are listed in Table I. There is an uncertainty due to the decay time range used because of the possible change of the acceptance ratio at short decay times. This uncertainty is ascertained by changing the fit range to be 1–7 ps and using the difference with the baseline fit. To determine the acceptance slope uncertainty we vary the value of a by its error determined from the fit to the simulation samples and propagate this change to the results. For the signal shape uncertainty, we repeat the measurement of $\Delta_{\Lambda B}$ using a double-Gaussian signal shape in the mass fits. The uncertainty in the background parametrization is assigned by letting the background parameters vary in the fits to the time dependent yields and comparing the difference in final results. Effects of changes in the acceptance for the Λ_b^0 mode due to the angular decay distributions are evaluated by weighting the simulation by the observed pK^- helicity angle in addition to the pK^- invariant mass, and redoing the analysis. The acceptance function uncertainty is evaluated by using a parabola instead of a linear function. The total systematic uncertainty is obtained by adding all of the elements in quadrature.

In conclusion, our value for $\tau_{\Lambda_b^0}/\tau_{\bar{B}^0} = 0.976 \pm 0.012 \pm 0.006$ shows that the Λ_b^0 and $\bar{B}^0$ lifetimes are indeed equal to within a few percent, as the original advocates of the HQE claimed [3,4,9], without any need to find additional corrections. Adding both uncertainties in quadrature, the lifetimes are consistent with being equal at the level of 1.9 standard deviations; thus, we do not exclude that the Λ_b^0 baryon has a longer lifetime than the $\bar{B}^0$ meson. Using the world average measured value for the $\bar{B}^0$ lifetime, we determine $\tau_{\Lambda_b^0} = 1.482 \pm 0.018 \pm 0.012$ ps.

We are thankful for many useful and interesting conversations with Prof. Nikolai Uraltsev (now deceased) who contributed greatly to theories describing heavy hadron lifetimes. We express our gratitude to our colleagues in the CERN accelerator departments for the excellent performance of the LHC. We thank the technical and administrative staff at the LHCb institutes. We acknowledge

support from CERN and from the national agencies: CAPES, CNPq, FAPERJ, and FINEP (Brazil); NSFC (China); CNRS/IN2P3 and Region Auvergne (France); BMBF, DFG, HGF, and MPG (Germany); SFI (Ireland); INFN (Italy); FOM and NWO (Netherlands); SCSR (Poland); MEN/IFA (Romania); MinES, Rosatom, RFBR, and NRC "Kurchatov Institute" (Russia); MinECo, XuntaGal, and GENCAT (Spain); SNSF and SER (Switzerland); NAS Ukraine (Ukraine); STFC (United Kingdom); NSF (USA). We also acknowledge the support received from the ERC under FP7. The Tier1 computing centres are supported by IN2P3 (France), KIT and BMBF (Germany), INFN (Italy), NWO and SURF (Netherlands), PIC (Spain), GridPP (United Kingdom). We are thankful for the computing resources put at our disposal by Yandex LLC (Russia), as well as to the communities behind the multiple open source software packages that we depend on.

[1] R. Kowalewski and T. Mannel, Phys. Rev. D **86**, 010001 (2012); F. U. Bernlochner *et al.*, Proc. Sci. ICHEP2010 (2010) 229 [arXiv:1011.5838].
[2] J. Laiho, E. Lunghi, and R. Van de Water, Proc. Sci. LATTICE2011 (2011) 018 [arXiv:1204.0791]; S. Stone, arXiv:1212.6374.
[3] I. I. Bigi, arXiv:hep-ph/9508408; I. I. Bigi *et al.*, in *B Decays*, edited by S. Stone (World Scientific, Singapore, 1994).
[4] N. Uraltsev, arXiv:hep-ph/9804275.
[5] M. Neubert, Adv. Ser. Dir. High Energy Phys. **15**, 239 (1998).
[6] K. Wilson and W. Zimmermann, Commun. Math. Phys. **24**, 87 (1972); G. Buchalla, A. J. Buras, and M. E. Lautenbacher, Rev. Mod. Phys. **68**, 1125 (1996).
[7] A. F. Falk, arXiv:hep-ph/0007339; A. J. Buras, arXiv:1102.5650.
[8] H.-Y. Cheng, Phys. Rev. D **56**, 2783 (1997).
[9] M. Neubert and C. T. Sachrajda, Nucl. Phys. **B483**, 339 (1997).
[10] N. Uraltsev, Phys. Lett. B **376**, 303 (1996); M. Di Pierro, C. T. Sachrajda, and C. Michael (UKQCD Collaboration), Phys. Lett. B **468**, 143 (1999).
[11] J. L. Rosner, Phys. Lett. B **379**, 267 (1996).
[12] M. Battaglia *et al.*, arXiv:hep-ph/0304132.
[13] C. Tarantino, Eur. Phys. J. C **33**, S895 (2004); E. Franco, V. Lubicz, F. Mescia, and C. Tarantino, Nucl. Phys. **B633**, 212 (2002).
[14] T. Ito, M. Matsuda, and Y. Matsui, Prog. Theor. Phys. **99**, 271 (1998); F. Gabbiani, A. I. Onishchenko, and A. A. Petrov, Phys. Rev. D **68**, 114006 (2003); **70**, 094031 (2004).
[15] N. Uraltsev, arXiv:hep-ph/0010328.
[16] G. Aad *et al.* (ATLAS Collaboration), Phys. Rev. D **87**, 032002 (2013); S. Chatrchyan *et al.* (CMS Collaboration), arXiv:1304.7495; T. Aaltonen *et al.* (CDF Collaboration), Phys. Rev. Lett. **104**, 102002 (2010); T. Aaltonen *et al.* (CDF Collaboration), Phys. Rev. Lett. **106**, 121804 (2011); V. M. Abazov *et al.* (D0 Collaboration), Phys. Rev. D **85**, 112003 (2012).
[17] A. Alves, Jr. *et al.* (LHCb Collaboration), JINST **3**, S08005 (2008).
[18] R. Aaij *et al.*, JINST **8**, P04022 (2013).
[19] T. Sjöstrand, S. Mrenna, and P. Z. Skands, J. High Energy Phys. 05 (2006) 026; I. Belyaev *et al.*, in *Nuclear Science Symposium Conference Record (NSS/MIC) 2010 IEEE 2010* (IEEE, Piscataway, NJ, 2010) p. 1155; S. Agostinelli *et al.* (GEANT4 Collaboration), Nucl. Instrum. Methods Phys. Res., Sect. A **506**, 250 (2003); J. Allison *et al.* (GEANT4 Collaboration), IEEE Trans. Nucl. Sci. **53**, 270 (2006); M. Clemencic, G. Corti, S. Easo, C. R. Jones, S. Miglioranzi, M. Pappagallo, and P. Robbe, J. Phys. Conf. Ser. **331**, 032023 (2011); D. Lange, Nucl. Instrum. Methods Phys. Res., Sect. A **462**, 152 (2001).
[20] L. Breiman, J. H. Friedman, R. A. Olshen, and C. J. Stone, *Classification and Regression Trees* (Wadsworth International Group, Belmont, California, 1984).
[21] M. Adinolfi *et al.*, Eur. Phys. J. C **73**, 2431 (2013).
[22] R. Aaij *et al.* (LHCb Collaboration), Phys. Rev. D **87**, 072004 (2013).
[23] J. Beringer *et al.* (Particle Data Group), Phys. Rev. D **86**, 010001 (2012), and 2013 partial update for the 2014 edition.

R. Aaij,[40] B. Adeva,[36] M. Adinolfi,[45] C. Adrover,[6] A. Affolder,[51] Z. Ajaltouni,[5] J. Albrecht,[9] F. Alessio,[37] M. Alexander,[50] S. Ali,[40] G. Alkhazov,[29] P. Alvarez Cartelle,[36] A. A. Alves, Jr.,[24,37] S. Amato,[2] S. Amerio,[21] Y. Amhis,[7] L. Anderlini,[17,f] J. Anderson,[39] R. Andreassen,[56] J. E. Andrews,[57] R. B. Appleby,[53] O. Aquines Gutierrez,[10] F. Archilli,[18] A. Artamonov,[34] M. Artuso,[58] E. Aslanides,[6] G. Auriemma,[24,m] M. Baalouch,[5] S. Bachmann,[11] J. J. Back,[47] C. Baesso,[59] V. Balagura,[30] W. Baldini,[16] R. J. Barlow,[53] C. Barschel,[37] S. Barsuk,[7] W. Barter,[46] Th. Bauer,[40] A. Bay,[38] J. Beddow,[50] F. Bedeschi,[22] I. Bediaga,[1] S. Belogurov,[30] K. Belous,[34] I. Belyaev,[30] E. Ben-Haim,[8] G. Bencivenni,[18] S. Benson,[49] J. Benton,[45] A. Berezhnoy,[31] R. Bernet,[39] M.-O. Bettler,[46] M. van Beuzekom,[40] A. Bien,[11] S. Bifani,[44] T. Bird,[53] A. Bizzeti,[17,h] P. M. Bjørnstad,[53] T. Blake,[37] F. Blanc,[38] J. Blouw,[11] S. Blusk,[58] V. Bocci,[24] A. Bondar,[33] N. Bondar,[29] W. Bonivento,[15] S. Borghi,[53] A. Borgia,[58] T. J. V. Bowcock,[51] E. Bowen,[39] C. Bozzi,[16] T. Brambach,[9] J. van den Brand,[41] J. Bressieux,[38] D. Brett,[53] M. Britsch,[10] T. Britton,[58] N. H. Brook,[45] H. Brown,[51] I. Burducea,[28] A. Bursche,[39] G. Busetto,[21,q] J. Buytaert,[37] S. Cadeddu,[15] O. Callot,[7] M. Calvi,[20,j] M. Calvo Gomez,[35,n] A. Camboni,[35] P. Campana,[18,37] D. Campora Perez,[37]

A. Carbone,[14,c] G. Carboni,[23,k] R. Cardinale,[19,i] A. Cardini,[15] H. Carranza-Mejia,[49] L. Carson,[52] K. Carvalho Akiba,[2] G. Casse,[51] L. Castillo Garcia,[37] M. Cattaneo,[37] Ch. Cauet,[9] R. Cenci,[57] M. Charles,[54] Ph. Charpentier,[37] P. Chen,[3,38] N. Chiapolini,[39] M. Chrzaszcz,[25] K. Ciba,[37] X. Cid Vidal,[37] G. Ciezarek,[52] P. E. L. Clarke,[49] M. Clemencic,[37] H. V. Cliff,[46] J. Closier,[37] C. Coca,[28] V. Coco,[40] J. Cogan,[6] E. Cogneras,[5] P. Collins,[37] A. Comerma-Montells,[35] A. Contu,[15,37] A. Cook,[45] M. Coombes,[45] S. Coquereau,[8] G. Corti,[37] B. Couturier,[37] G. A. Cowan,[49] D. C. Craik,[47] S. Cunliffe,[52] R. Currie,[49] C. D'Ambrosio,[37] P. David,[8] P. N. Y. David,[40] A. Davis,[56] I. De Bonis,[4] K. De Bruyn,[40] S. De Capua,[53] M. De Cian,[11] J. M. De Miranda,[1] L. De Paula,[2] W. De Silva,[56] P. De Simone,[18] D. Decamp,[4] M. Deckenhoff,[9] L. Del Buono,[8] N. Déléage,[4] D. Derkach,[54] O. Deschamps,[5] F. Dettori,[41] A. Di Canto,[11] H. Dijkstra,[37] M. Dogaru,[28] S. Donleavy,[51] F. Dordei,[11] A. Dosil Suárez,[36] D. Dossett,[47] A. Dovbnya,[42] F. Dupertuis,[38] P. Durante,[37] R. Dzhelyadin,[34] A. Dziurda,[25] A. Dzyuba,[29] S. Easo,[48] U. Egede,[52] V. Egorychev,[30] S. Eidelman,[33] D. van Eijk,[40] S. Eisenhardt,[49] U. Eitschberger,[9] R. Ekelhof,[9] L. Eklund,[50,37] I. El Rifai,[5] Ch. Elsasser,[39] A. Falabella,[14,e] C. Färber,[11] G. Fardell,[49] C. Farinelli,[40] S. Farry,[51] D. Ferguson,[49] V. Fernandez Albor,[36] F. Ferreira Rodrigues,[1] M. Ferro-Luzzi,[37] S. Filippov,[32] M. Fiore,[16] C. Fitzpatrick,[37] M. Fontana,[10] F. Fontanelli,[19,i] R. Forty,[37] O. Francisco,[2] M. Frank,[37] C. Frei,[37] M. Frosini,[17,f] S. Furcas,[20] E. Furfaro,[23,k] A. Gallas Torreira,[36] D. Galli,[14,c] M. Gandelman,[2] P. Gandini,[58] Y. Gao,[3] J. Garofoli,[58] P. Garosi,[53] J. Garra Tico,[46] L. Garrido,[35] C. Gaspar,[37] R. Gauld,[54] E. Gersabeck,[11] M. Gersabeck,[53] T. Gershon,[47,37] Ph. Ghez,[4] V. Gibson,[46] L. Giubega,[28] V. V. Gligorov,[37] C. Göbel,[59] D. Golubkov,[30] A. Golutvin,[52,30,37] A. Gomes,[2] P. Gorbounov,[30,37] H. Gordon,[54] M. Grabalosa Gándara,[5] R. Graciani Diaz,[35] L. A. Granado Cardoso,[37] E. Graugés,[35] G. Graziani,[17] A. Grecu,[28] E. Greening,[54] S. Gregson,[46] P. Griffith,[44] O. Grünberg,[60] B. Gui,[58] E. Gushchin,[32] Yu. Guz,[34,37] T. Gys,[37] C. Hadjivasiliou,[58] G. Haefeli,[38] C. Haen,[37] S. C. Haines,[46] S. Hall,[52] B. Hamilton,[57] T. Hampson,[45] S. Hansmann-Menzemer,[11] N. Harnew,[54] S. T. Harnew,[45] J. Harrison,[53] T. Hartmann,[60] J. He,[37] T. Head,[37] V. Heijne,[40] K. Hennessy,[51] P. Henrard,[5] J. A. Hernando Morata,[36] E. van Herwijnen,[37] A. Hicheur,[1] E. Hicks,[51] D. Hill,[54] M. Hoballah,[5] C. Hombach,[53] P. Hopchev,[4] W. Hulsbergen,[40] P. Hunt,[54] T. Huse,[51] N. Hussain,[54] D. Hutchcroft,[51] D. Hynds,[50] V. Iakovenko,[43] M. Idzik,[26] P. Ilten,[12] R. Jacobsson,[37] A. Jaeger,[11] E. Jans,[40] P. Jaton,[38] A. Jawahery,[57] F. Jing,[3] M. John,[54] D. Johnson,[54] C. R. Jones,[46] C. Joram,[37] B. Jost,[37] M. Kaballo,[9] S. Kandybei,[42] W. Kanso,[6] M. Karacson,[37] T. M. Karbach,[37] I. R. Kenyon,[44] T. Ketel,[41] A. Keune,[38] B. Khanji,[20] O. Kochebina,[7] I. Komarov,[38] R. F. Koopman,[41] P. Koppenburg,[40] M. Korolev,[31] A. Kozlinskiy,[40] L. Kravchuk,[32] K. Kreplin,[11] M. Kreps,[47] G. Krocker,[11] P. Krokovny,[33] F. Kruse,[9] M. Kucharczyk,[20,25,j] V. Kudryavtsev,[33] T. Kvaratskheliya,[30,37] V. N. La Thi,[38] D. Lacarrere,[37] G. Lafferty,[53] A. Lai,[15] D. Lambert,[49] R. W. Lambert,[41] E. Lanciotti,[37] G. Lanfranchi,[18] C. Langenbruch,[37] T. Latham,[47] C. Lazzeroni,[44] R. Le Gac,[6] J. van Leerdam,[40] J.-P. Lees,[4] R. Lefèvre,[5] A. Leflat,[31] J. Lefrançois,[7] S. Leo,[22] O. Leroy,[6] T. Lesiak,[25] B. Leverington,[11] Y. Li,[3] L. Li Gioi,[5] M. Liles,[51] R. Lindner,[37] C. Linn,[11] B. Liu,[3] G. Liu,[37] S. Lohn,[37] I. Longstaff,[50] J. H. Lopes,[2] N. Lopez-March,[38] H. Lu,[3] D. Lucchesi,[21,q] J. Luisier,[38] H. Luo,[49] F. Machefert,[7] I. V. Machikhiliyan,[4,30] F. Maciuc,[28] O. Maev,[29,37] S. Malde,[54] G. Manca,[15,d] G. Mancinelli,[6] J. Maratas,[5] U. Marconi,[14] P. Marino,[22,s] R. Märki,[38] J. Marks,[11] G. Martellotti,[24] A. Martens,[8] A. Martín Sánchez,[7] M. Martinelli,[40] D. Martinez Santos,[41] D. Martins Tostes,[2] A. Massafferri,[1] R. Matev,[37] Z. Mathe,[37] C. Matteuzzi,[20] E. Maurice,[6] A. Mazurov,[16,32,37,e] B. Mc Skelly,[51] J. McCarthy,[44] A. McNab,[53] R. McNulty,[12] B. Meadows,[56,54] F. Meier,[9] M. Meissner,[11] M. Merk,[40] D. A. Milanes,[8] M.-N. Minard,[4] J. Molina Rodriguez,[59] S. Monteil,[5] D. Moran,[53] P. Morawski,[25] A. Mordà,[6] M. J. Morello,[22,s] R. Mountain,[58] I. Mous,[40] F. Muheim,[49] K. Müller,[39] R. Muresan,[28] B. Muryn,[26] B. Muster,[38] P. Naik,[45] T. Nakada,[38] R. Nandakumar,[48] I. Nasteva,[1] M. Needham,[49] S. Neubert,[37] N. Neufeld,[37] A. D. Nguyen,[38] T. D. Nguyen,[38] C. Nguyen-Mau,[38,o] M. Nicol,[7] V. Niess,[5] R. Niet,[9] N. Nikitin,[31] T. Nikodem,[11] A. Nomerotski,[54] A. Novoselov,[34] A. Oblakowska-Mucha,[26] V. Obraztsov,[34] S. Oggero,[40] S. Ogilvy,[50] O. Okhrimenko,[43] R. Oldeman,[15,d] M. Orlandea,[28] J. M. Otalora Goicochea,[2] P. Owen,[52] A. Oyanguren,[35] B. K. Pal,[58] A. Palano,[13,b] T. Palczewski,[27] M. Palutan,[18] J. Panman,[37] A. Papanestis,[48] M. Pappagallo,[50] C. Parkes,[53] C. J. Parkinson,[52] G. Passaleva,[17] G. D. Patel,[51] M. Patel,[52] G. N. Patrick,[48] C. Patrignani,[19,i] C. Pavel-Nicorescu,[28] A. Pazos Alvarez,[36] A. Pellegrino,[40] G. Penso,[24,l] M. Pepe Altarelli,[37] S. Perazzini,[14,c] E. Perez Trigo,[36] A. Pérez-Calero Yzquierdo,[35] P. Perret,[5] M. Perrin-Terrin,[6] L. Pescatore,[44] E. Pesen,[61] G. Pessina,[20] K. Petridis,[52] A. Petrolini,[19,i] A. Phan,[58] E. Picatoste Olloqui,[35] B. Pietrzyk,[4] T. Pilař,[47] D. Pinci,[24] S. Playfer,[49] M. Plo Casasus,[36] F. Polci,[8] G. Polok,[25] A. Poluektov,[47,33] E. Polycarpo,[2] A. Popov,[34] D. Popov,[10] B. Popovici,[28] C. Potterat,[35] A. Powell,[54] J. Prisciandaro,[38] A. Pritchard,[51] C. Prouve,[7] V. Pugatch,[43] A. Puig Navarro,[38] G. Punzi,[22,r] W. Qian,[4] J. H. Rademacker,[45] B. Rakotomiaramanana,[38] M. S. Rangel,[2] I. Raniuk,[42]

N. Rauschmayr,[37] G. Raven,[41] S. Redford,[54] M. M. Reid,[47] A. C. dos Reis,[1] S. Ricciardi,[48] A. Richards,[52] K. Rinnert,[51] V. Rives Molina,[35] D. A. Roa Romero,[5] P. Robbe,[7] D. A. Roberts,[57] E. Rodrigues,[53] P. Rodriguez Perez,[36] S. Roiser,[37] V. Romanovsky,[34] A. Romero Vidal,[36] J. Rouvinet,[38] T. Ruf,[37] F. Ruffini,[22] H. Ruiz,[35] P. Ruiz Valls,[35] G. Sabatino,[24,k] J. J. Saborido Silva,[36] N. Sagidova,[29] P. Sail,[50] B. Saitta,[15,d] V. Salustino Guimaraes,[2] B. Sanmartin Sedes,[36] M. Sannino,[19,i] R. Santacesaria,[24] C. Santamarina Rios,[36] E. Santovetti,[23,k] M. Sapunov,[6] A. Sarti,[18,l] C. Satriano,[24,m] A. Satta,[23] M. Savrie,[16,e] D. Savrina,[30,31] P. Schaack,[52] M. Schiller,[41] H. Schindler,[37] M. Schlupp,[9] M. Schmelling,[10] B. Schmidt,[37] O. Schneider,[38] A. Schopper,[37] M.-H. Schune,[7] R. Schwemmer,[37] B. Sciascia,[18] A. Sciubba,[24] M. Seco,[36] A. Semennikov,[30] K. Senderowska,[26] I. Sepp,[52] N. Serra,[39] J. Serrano,[6] P. Seyfert,[11] M. Shapkin,[34] I. Shapoval,[16,42] P. Shatalov,[30] Y. Shcheglov,[29] T. Shears,[51,37] L. Shekhtman,[33] O. Shevchenko,[42] V. Shevchenko,[30] A. Shires,[52] R. Silva Coutinho,[47] M. Sirendi,[46] T. Skwarnicki,[58] N. A. Smith,[51] E. Smith,[54,48] J. Smith,[46] M. Smith,[53] M. D. Sokoloff,[56] F. J. P. Soler,[50] F. Soomro,[18] D. Souza,[45] B. Souza De Paula,[2] B. Spaan,[9] A. Sparkes,[49] P. Spradlin,[50] F. Stagni,[37] S. Stahl,[11] O. Steinkamp,[39] S. Stevenson,[54] S. Stoica,[28] S. Stone,[58] B. Storaci,[39] M. Straticiuc,[28] U. Straumann,[39] V. K. Subbiah,[37] L. Sun,[56] S. Swientek,[9] V. Syropoulos,[41] M. Szczekowski,[27] P. Szczypka,[38,37] T. Szumlak,[26] S. T'Jampens,[4] M. Teklishyn,[7] E. Teodorescu,[28] F. Teubert,[37] C. Thomas,[54] E. Thomas,[37] J. van Tilburg,[11] V. Tisserand,[4] M. Tobin,[38] S. Tolk,[41] D. Tonelli,[37] S. Topp-Joergensen,[54] N. Torr,[54] E. Tournefier,[4,52] S. Tourneur,[38] M. T. Tran,[38] M. Tresch,[39] A. Tsaregorodtsev,[6] P. Tsopelas,[40] N. Tuning,[40] M. Ubeda Garcia,[37] A. Ukleja,[27] D. Urner,[53] A. Ustyuzhanin,[52,p] U. Uwer,[11] V. Vagnoni,[14] G. Valenti,[14] A. Vallier,[7] M. Van Dijk,[45] R. Vazquez Gomez,[18] P. Vazquez Regueiro,[36] C. Vázquez Sierra,[36] S. Vecchi,[16] J. J. Velthuis,[45] M. Veltri,[17,g] G. Veneziano,[38] M. Vesterinen,[37] B. Viaud,[7] D. Vieira,[2] X. Vilasis-Cardona,[35,n] A. Vollhardt,[39] D. Volyanskyy,[10] D. Voong,[45] A. Vorobyev,[29] V. Vorobyev,[33] C. Voß,[60] H. Voss,[10] R. Waldi,[60] C. Wallace,[47] R. Wallace,[12] S. Wandernoth,[11] J. Wang,[58] D. R. Ward,[46] N. K. Watson,[44] A. D. Webber,[53] D. Websdale,[52] M. Whitehead,[47] J. Wicht,[37] J. Wiechczynski,[25] D. Wiedner,[11] L. Wiggers,[40] G. Wilkinson,[54] M. P. Williams,[47,48] M. Williams,[55] F. F. Wilson,[48] J. Wimberley,[57] J. Wishahi,[9] W. Wislicki,[27] M. Witek,[25] S. A. Wotton,[46] S. Wright,[46] S. Wu,[3] K. Wyllie,[37] Y. Xie,[49,37] Z. Xing,[58] Z. Yang,[3] R. Young,[49] X. Yuan,[3] O. Yushchenko,[34] M. Zangoli,[14] M. Zavertyaev,[10,a] F. Zhang,[3] L. Zhang,[58] W. C. Zhang,[12] Y. Zhang,[3] A. Zhelezov,[11] A. Zhokhov,[30] L. Zhong,[3] and A. Zvyagin[37]

(LHCb Collaboration)

[1]*Centro Brasileiro de Pesquisas Físicas (CBPF), Rio de Janeiro, Brazil*
[2]*Universidade Federal do Rio de Janeiro (UFRJ), Rio de Janeiro, Brazil*
[3]*Center for High Energy Physics, Tsinghua University, Beijing, China*
[4]*LAPP, Université de Savoie, CNRS/IN2P3, Annecy-Le-Vieux, France*
[5]*Clermont Université, Université Blaise Pascal, CNRS/IN2P3, LPC, Clermont-Ferrand, France*
[6]*CPPM, Aix-Marseille Université, CNRS/IN2P3, Marseille, France*
[7]*LAL, Université Paris-Sud, CNRS/IN2P3, Orsay, France*
[8]*LPNHE, Université Pierre et Marie Curie, Université Paris Diderot, CNRS/IN2P3, Paris, France*
[9]*Fakultät Physik, Technische Universität Dortmund, Dortmund, Germany*
[10]*Max-Planck-Institut für Kernphysik (MPIK), Heidelberg, Germany*
[11]*Physikalisches Institut, Ruprecht-Karls-Universität Heidelberg, Heidelberg, Germany*
[12]*School of Physics, University College Dublin, Dublin, Ireland*
[13]*Sezione INFN di Bari, Bari, Italy*
[14]*Sezione INFN di Bologna, Bologna, Italy*
[15]*Sezione INFN di Cagliari, Cagliari, Italy*
[16]*Sezione INFN di Ferrara, Ferrara, Italy*
[17]*Sezione INFN di Firenze, Firenze, Italy*
[18]*Laboratori Nazionali dell'INFN di Frascati, Frascati, Italy*
[19]*Sezione INFN di Genova, Genova, Italy*
[20]*Sezione INFN di Milano Bicocca, Milano, Italy*
[21]*Sezione INFN di Padova, Padova, Italy*
[22]*Sezione INFN di Pisa, Pisa, Italy*
[23]*Sezione INFN di Roma Tor Vergata, Roma, Italy*
[24]*Sezione INFN di Roma La Sapienza, Roma, Italy*
[25]*Henryk Niewodniczanski Institute of Nuclear Physics Polish Academy of Sciences, Kraków, Poland*
[26]*Faculty of Physics and Applied Computer Science, AGH-University of Science and Technology, Kraków, Poland*

[27]National Center for Nuclear Research (NCBJ), Warsaw, Poland
[28]Horia Hulubei National Institute of Physics and Nuclear Engineering, Bucharest-Magurele, Romania
[29]Petersburg Nuclear Physics Institute (PNPI), Gatchina, Russia
[30]Institute of Theoretical and Experimental Physics (ITEP), Moscow, Russia
[31]Institute of Nuclear Physics, Moscow State University (SINP MSU), Moscow, Russia
[32]Institute for Nuclear Research of the Russian Academy of Sciences (INR RAN), Moscow, Russia
[33]Budker Institute of Nuclear Physics (SB RAS) and Novosibirsk State University, Novosibirsk, Russia
[34]Institute for High Energy Physics (IHEP), Protvino, Russia
[35]Universitat de Barcelona, Barcelona, Spain
[36]Universidad de Santiago de Compostela, Santiago de Compostela, Spain
[37]European Organization for Nuclear Research (CERN), Geneva, Switzerland
[38]Ecole Polytechnique Fédérale de Lausanne (EPFL), Lausanne, Switzerland
[39]Physik-Institut, Universität Zürich, Zürich, Switzerland
[40]Nikhef National Institute for Subatomic Physics, Amsterdam, Netherlands
[41]Nikhef National Institute for Subatomic Physics and VU University Amsterdam, Amsterdam, Netherlands
[42]NSC Kharkiv Institute of Physics and Technology (NSC KIPT), Kharkiv, Ukraine
[43]Institute for Nuclear Research of the National Academy of Sciences (KINR), Kyiv, Ukraine
[44]University of Birmingham, Birmingham, United Kingdom
[45]H. H. Wills Physics Laboratory, University of Bristol, Bristol, United Kingdom
[46]Cavendish Laboratory, University of Cambridge, Cambridge, United Kingdom
[47]Department of Physics, University of Warwick, Coventry, United Kingdom
[48]STFC Rutherford Appleton Laboratory, Didcot, United Kingdom
[49]School of Physics and Astronomy, University of Edinburgh, Edinburgh, United Kingdom
[50]School of Physics and Astronomy, University of Glasgow, Glasgow, United Kingdom
[51]Oliver Lodge Laboratory, University of Liverpool, Liverpool, United Kingdom
[52]Imperial College London, London, United Kingdom
[53]School of Physics and Astronomy, University of Manchester, Manchester, United Kingdom
[54]Department of Physics, University of Oxford, Oxford, United Kingdom
[55]Massachusetts Institute of Technology, Cambridge, Massachusetts 02139, USA
[56]University of Cincinnati, Cincinnati, Ohio 45221, USA
[57]University of Maryland, College Park, Maryland 20742, USA
[58]Syracuse University, Syracuse, New York 13224, USA
[59]Pontifícia Universidade Católica do Rio de Janeiro (PUC-Rio), Rio de Janeiro, Brazil [associated with Universidade Federal do Rio de Janeiro (UFRJ), Rio de Janeiro, Brazil]
[60]Institut für Physik, Universität Rostock, Rostock, Germany (associated with Physikalisches Institut, Ruprecht-Karls-Universität Heidelberg, Heidelberg, Germany)
[61]Celal Bayar University, Manisa, Turkey [associated with European Organization for Nuclear Research (CERN), Geneva, Switzerland]

[a]Also at P.N. Lebedev Physical Institute, Russian Academy of Science (LPI RAS), Moscow, Russia.
[b]Also at Università di Bari, Bari, Italy.
[c]Also at Università di Bologna, Bologna, Italy.
[d]Also at Università di Cagliari, Cagliari, Italy.
[e]Also at Università di Ferrara, Ferrara, Italy.
[f]Also at Università di Firenze, Firenze, Italy
[g]Also at Università di Urbino, Urbino, Italy.
[h]Also at Università di Modena e Reggio Emilia, Modena, Italy.
[i]Also at Università di Genova, Genova, Italy.
[j]Also at Università di Milano Bicocca, Milano, Italy.
[k]Also at Università di Roma Tor Vergata, Roma, Italy.
[l]Also at Università di Roma La Sapienza, Roma, Italy.
[m]Also at Università della Basilicata, Potenza, Italy.
[n]Also at LIFAELS, La Salle, Universitat Ramon Llull, Barcelona, Spain.
[o]Also at Hanoi University of Science, Hanoi, Viet Nam.
[p]Also at Institute of Physics and Technology, Moscow, Russia.
[q]Also at Università di Padova, Padova, Italy.
[r]Also at Università di Pisa, Pisa, Italy.
[s]Also at Scuola Normale Superiore, Pisa, Italy.